In Vivo Competition Studies with Analogues of 3-Quinuclidinyl Benzilate

WILLIAM C. ECKELMAN *§x, M. GRISSOM ‡, J. CONKLIN ‡, W. J. RZESZOTARSKI *, R. E. GIBSON *, B. E. FRANCIS *, E. M. JAGODA *, R. ENG ‡, and R. C. REBA *

Received December 16, 1982, from the *Section of Radiopharmaceutical Chemistry, The George Washington University Medical Center, Washington, DC 20037 and ‡Nuclear Sciences Division, Armed Forces Radiobiology Research Institute, Bethesda, MD 20814. Accepted for publication March 17, 1983. §Present address: National Institutes of Health, Building 10, Rm 1C488, Bethesda, MD 20205.

Abstract □ Among ligands that bind to the α- and β-adrenoceptors and to the muscarinic acetylcholine receptor (m-AChR), those that bind to the latter have the best properties for external detection of receptor sites by gamma-camera imaging. To develop the optimal radiotracer, nonradioactive analogues of 3-quinuclidinyl benzilate (I) were tested in *in vivo* displacement studies with (−)-[^{3}H]I to determine their ability to compete with (−)-[^{3}H]I for the muscarinic acetylcholine receptor. There is a linear correlation between the ability to compete with (−)-[^{3}H]I for the m-AChR and the affinity constant of the analogue as determined by *in vitro* assay, suggesting that the test is a valid indicator of *in vivo* distribution. One radioiodinated analogue, 3-quinuclidinyl *p*-iodobenzilate, bound to m-AChR in the heart and brain of rats.

Keyphrases □ 3-Quinuclidinyl benzilate—analogues, binding to α- and β-adrenoceptors and the muscarinic acetylcholine receptor, gamma-camera imaging □ Radioligand binding—3-quinuclidinyl benzilate analogues to the muscarinic acetylcholine receptor, gamma-camera imaging □ Radiotracers—development of 3-quinuclidinyl benzilate analogues for gamma-camera imaging, binding to α- and β-adrenoceptors and muscarinic acetylcholine receptor

We have attempted to develop an effective strategy for the design, synthesis, *in vitro* analysis, animal distribution studies, and clinical evaluation of receptor binding radiotracers. Because of the special requirements for receptor binding radiotracers (high effective specific activity, high chemical and radiochemical purity, low nonreceptor binding, and low rate of metabolism) the choice is crucial (1). A large investment of research effort is needed to produce a radiolabeled receptor-binding ligand; only one receptor-binding radiotracer, 16α-[^{77}Br]bromoestradiol, is presently in the clinical trial phase (2)*.

To prepare a gamma-emitting receptor-binding radiotracer we have investigated several tritium-labeled compounds that bind to the α- and β-adrenoceptor and to the muscarinic acetylcholine receptor (m-AChR). The results, both *in vitro* and *in vivo*, using the tritium-labeled compounds led us to synthesize a number of nonradioactive derivatives of I substituted with stable isotopes of the routinely used gamma-emitting radionuclides iodine-123, bromine-77 and -75, and fluorine-18 (3). These stable halogenated derivatives of I were used in *in vivo* competition studies with (−)-[^{3}H]I to determine their ability to compete with the parent structure for m-AChR and, thus, give an indication of their own distribution.

Because making each derivative with iodine-123, bromine-77, or fluorine-18 would be an overwhelming task given the requirements mentioned previously, we thought that this approach—*in vivo* competition studies—would be an efficient strategy to determine which radiotracer to pursue. We also prepared and tested a number of other receptor-binding ligands to determine the structural requirements for binding to the receptor.

EXPERIMENTAL

Radioligands—(−)-3-[^{3}H]Quinuclidinyl benzilate (I)[1], (±)-4-(3-*tert*-butylamino-2-hydroxypropoxy)-1-*H*-2-cyano-3-[^{125}I]iodoindole (II)[2], and [^{3}H]prazosin (III)[1] were used without further purification. (±)-4-(3-*tert*-Butylamino-2-hydroxypropoxy)-1-*H*-3-[^{125}I]iodoindole (IV) was prepared according to the method of Barovsky and Brooker (4). Each was determined to be >95% radiochemically pure.

Preparation of Nonradioactive Compounds—*N*-Methyl scopolamine (V)[3], scopolamine (VI)[3], benactyzine (VII)[4], α-(hydroxymethyl) 4-bromobenzeneacetic acid 8-methyl-8-azabicyclo[3.2.1]oct-3-yl ester (4-bromoatropine; VIII)[5], benztropine (IX)[6], carbetapentane (X)[7], carazolol (XI)[8], phentolamine (XII)[9], propranolol (XIII)[10], and pindolol (XIV)[11] were obtained commercially. Other compounds were prepared and purified as previously published (3). Each derivative (3 μmol) was dissolved in 3 mL of EtOH without heat. At the time of use, 3 mL of saline was added, and 2 mL of this solution was mixed with 0.075–0.100 mL of (−)-[^{3}H]I at a final concentration of 37–50 μCi/mL. A 0.1-mL aliquot was injected per animal. Each compound was analyzed by HPLC before and after use by published techniques (3) and found to be chemically pure. Each analogue of I is a mixture of the four diastereomers.

Animal Studies—The *in vivo* distribution was determined in male Sprague–Dawley rats weighing 250–300 g at the time of study. The thyroid was not blocked. Under light halothane anesthesia, 0.1 mL of radiopharmaceutical solution (3–5 μCi in 50% ethanol) was injected into an exposed femoral vein. At selected times after the injection, the animals were killed and samples of blood, ventricular muscle, lung, liver, pancreas, midbrain, and cerebellum tissues were taken. The midbrain included the corpus striatum and hippocampus along with a portion of the brain stem. No cerebral cortex or pineal gland tissue was sampled. Small samples of solid tissue (100–200 mg) and blood (25 μL) were processed overnight in tissue solubilizer and then counted after the addition of liquid scintillation cocktail. Replicate counts separated by 24 h were taken to verify the absence of chemiluminescence. The results are expressed as the percentage of the injected dose per gram of wet tissue with 95% confidence limits. This allows direct comparison to determine if differences are significant at the 95% level.

RESULTS AND DISCUSSION

From our previous survey of various receptor systems in the heart such as the α- and β-adrenoceptors and the muscarinic acetylcholine receptor (m-AChR), it became obvious that the m-AChR system has the greatest potential. From a simple biomolecular model (5) and from distribution studies using commercially available tritium-labeled ligands, 3-quinuclidinyl benzilate (I) appeared to be the best radioligand (6).

Distribution of α- and β-Adrenoceptor Binding Radiotracer—The high-affinity β-adrenoceptor ligand XI and the high affinity α-adrenoceptor ligand III showed displaceable binding in the rat heart and lung, but XI gave

[1] New England Nuclear, Boston, Mass.
[2] ^{125}ICYP; Amersham, Arlington Height, Ill.
[3] Sigma Chemical Co., St.Louis, Mo.
[4] Aldrich Chemical Co., Milwaukee, Wis.
[5] 4-Bromoatropine; Smith Kline and French, Philadelphia, Pa.
[6] Merck Sharp & Dohme, West Point, Pa.
[7] Armour Pharmaceutical, Phoenix, Ariz.
[8] Boehringer Mannheim GmbH, Mannheim, West Germany.
[9] CIBA Pharmaceutical Co., Summit, N.J.
[10] Ayerst Lab Inc., New York, N.Y.
[11] Sandoz Pharmaceutical Laboratories, Hanover, N.J.

* Note added in proof: Two additional studies in humans have appeared: H. N. Wagner, Jr., H. D. Burns, R. F. Daniels, *et al.*, *Science*, **221**, 1262 (1983) and W. C. Eckelman, R. C. Reba, W. J. Rzeszotarski *et al.*, *Science*, **223**, 291 (1984).

0022-3549/84/0400-0529$01.00/0

Table I—Distribution of Selected α- and β-Adrenoceptor Radioligands in the Rat

	Time, h	Percent of Dose/g (95% Confidence Limits) Blood	Lung	Heart	Liver	Midbrain
[^{3}H]III						
Alone	2	0.052 (0.039–0.065)	0.301 (0.285–0.317)	0.880 (0.703–1.06)	1.80 (1.68–1.92)	0.056 (0.051–0.061)
+ 530 nmol of XII[a]	2	0.076 (0.071–0.082)	0.234 (0.206–0.263)	0.464 (0.441–0.487)	1.96 (1.71–2.21)	0.055 (0.049–0.061)
[^{3}H]XI						
Alone	2	0.175 (0.158–0.193)	4.49 (3.50–5.48)	0.392 (0.339–0.446)	0.525 (0.440–0.610)	0.090 (0.075–0.107)
+ 100 nmol of XIII[a]	2	0.097 (0.086–0.107)	1.26 (1.07–1.44)	0.201 (0.184–0.218)	0.497 (0.432–0.566)	0.080 (0.066–0.094)
[^{125}I]IV	0.25	0.494 (0.450–0.538)	2.09 (1.62–2.57)	0.326 (0.295–0.357)	—	0.054 (0.042–0.067)
	2	0.322 (0.283–0.361)	0.501 (0.371–0.632)	0.132 (0.106–0.158)	—	0.031 (0.026–0.036)
[^{125}I]II						
Alone	0.25	0.178 (0.137–0.220)	5.14 (2.40–7.88)	0.949 (0.606–1.29)	0.560 (0.334–0.787)	0.020 (0.012–0.029)
+ 100 nmol of XIV[a]	0.25	0.067 (0.053–0.080)	1.25 (0.627–1.87)	0.844 (0.380–1.31)	0.647 (0.355–0.939)	0.013 (0.001–0.024)
Alone	2	0.169 (0.139–0.199)	5.68 (5.00–6.38)	0.638 (0.498–0.777)	0.178 (0.149–0.207)	0.016 (0.012–0.020)
+ 100 nmol of XIV[a]	2	0.062 (0.052–0.069)	0.658 (0.532–0.785)	0.139 (0.108–0.168)	0.243 (0.204–0.283)	0.012 (0.007–0.018)

[a] Amount of nonradioactive compound coinjected per animal, six animals per group.

heart-to-blood (H/B) ratios of <5 (Table I) and III was not displaceable in guinea pig and rabbit (6). (±)-[^{3}H]I showed H/B ratios of >25 and displaceable binding in two species (6, 7).

Recently, three iodinated β-adrenoceptor ligands became available commercially. The first, iodohydroxybenzylpindolol (XV) gave low H/B ratios but displaceable binding in the lung (6). Two other compounds, II and IV, have also been prepared (8). Compound IV does not give high H/B ratios in the rat, but II does and also shows displaceable binding in the heart and lung (Table I). This compound appears to be useful for studying the change in concentration of β-adrenoceptors in both the heart and lung.

Very little uptake in the midbrain is observed so that this interesting location of α- and β-adrenoceptors cannot be studied with these agents (Table I). (−)-[^{3}H]I, on the other hand, shows not only high displaceable binding in the heart but also in the striatum (9). There is, therefore, an opportunity to study the change in m-AChR in these tissues if an appropriate gamma-emitting analogue of I can be prepared.

Proof of m-AChR Binding—The binding of (−)-[^{3}H]I to m-AChR in the heart and brain *in vitro* has been well documented. The burden of proof for m-AChR binding is based on the pharmacological profile whereby various agonists and antagonists are used in the *in vitro* assay, and the relative binding affinities are compared with physiological responses (10–13). We have added to this another test of binding to the m-AChR: stereospecificity. *In vitro*, the *R* and *S* isomers of I were shown to have affinity constants that differ by a factor of 58 in caudate putamen and 153 in ventricular muscle preparations (Table II). The evidence that (−)-[^{3}H]I is binding to the m-AChR *in vivo* is shown by the difference in competition of (−)-[^{3}H]I by the *R* and *S* isomers of I (Table III). The specific receptor binding relative to the nonreceptor binding can be determined in each case by comparing the concentration of (−)-[^{3}H]I in the presence and absence of an excess of competing nonradioactive ligand. Again the competition appeared to be stereoselective, with the more active isomer causing the greater displacement. We therefore conclude that we are studying binding to the m-AChR both *in vitro* and *in vivo*.

Table II—Relative Binding Index (RBI) of Derivatives of I[a]

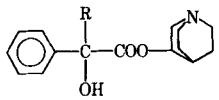

R	RBI Heart	Midbrain
C_6H_5	100	100
c-C_5H_9	155	99
c-C_6H_{11}	66	70
n-C_4H_9	55	95
4-FC_6H_4	57	110
3-FC_6H_4	95	116
4-BrC_6H_4	11	69
3-BrC_6H_4	8	84
2-BrC_6H_4	8	18
4-IC_6H_4	23	65
3-IC_6H_4	9	32
4-$NH_2C_6H_4$	6	16
(*R*)-C_6H_5	184	230
(*S*)-C_6H_5	2	4
Propargyl	1	3
C_6H_5, *N*-methyl	15	—
3-Quinuclidinyl xanthene-9-carboxylate	4	98
Atropine	3	20
Scopolamine	3	22

[a] Calculated from data in Refs. 3 and 11. The RBI is the affinity constant of each compound relative to that of (±)-I as determined by *in vitro* assay where (±)-I is 100.

Competitive Binding of Muscarinic Antagonist—Fifty nmole of each halogen analogue of I was coinjected with (−)-[^{3}H]I to determine the distribution of these nonradioactive derivatives indirectly. In the heart and midbrain the fluoro analogues are the most potent, followed by the bromo analogues, and finally the iodo analogues (Table III).

We also prepared a number of alkyl derivatives that contain a cyclohexyl, a cyclopentyl, or an *n*-butyl group in place of one aromatic ring (3) (Table IV). The cyclopentyl derivative has a higher affinity than I for the m-AChR in the heart, and this is reflected in the *in vivo* competition study (Fig. 1). This study shows that these structural changes do not adversely affect *in vivo* m-AChR binding and indicates alternate pathways to radiolabeling.

The remaining compounds are drugs that are thought to interact with the m-AChR (Table V). Compound VI is used for the relief of pylorospasm, peptic ulcer, and spastic colon. It is not as effective as I in inhibiting (−)-[^{3}H]I. The *N*-methyl quaternary derivative (V) is more potent than VI in *in vivo* displacement in the heart, but does not displace (−)-[^{3}H]I in the brain because the quaternary salt does not cross the blood–brain barrier. Compound VII is a mild antidepressant and anticholinergic agent; from the *in vivo* displacement studies it is indeed a weak displacer. Likewise VIII, a halogenated derivative of atropine, IX, an anticholinergic and antihistaminic derivative of tropine, and X, a sympathomimetic agent used in cough medicine, all are weak inhibitors of (−)-[^{3}H]I binding in all organs studied.

Correlation of *In Vitro* and *In Vivo* Results—These values for competitive blockade are in general agreement with the affinity constants determined by *in vitro* assay in our laboratory (Table II). The *in vitro* relative binding affinity was correlated with the *in vivo* displacement data using the logit–log plot (Fig. 1) (14). The logit–log plot was chosen because it uses experimental values, *i.e.*, B/B_0 (the amount of (−)-[^{3}H]I bound in the presence of nonradioactive inhibitor divided by the amount bound in the absence of inhibitor) and usually the log of the concentration of inhibitor (h):

$$\text{Logit } B/B_0 = -\log h - \log \frac{K_h}{1 + K_a L_0} \qquad \text{(Eq. 1)}$$

Since in our case the amount of (−)-[^{3}H]I injected (L_0), the affinity (K_a), and h are constant, we have chosen to plot the log of the relative binding index

Table III—Displacement of (−)-[^{3}H]I by I and Halogenated Derivatives at 2 h in the Rat

Derivative (R)[a]	Percent of Dose/g (95% Confidence Limits)					
	Blood	Lung	Heart	Liver	Midbrain	Cerebellum
3-FC_6H_4	0.085 (0.079–0.091)	0.285 (0.226–0.344)	0.284 (0.263–0.305)	0.270 (0.244–0.297)	0.508 (0.418–0.598)	0.164 (0.153–0.175)
4-FC_6H_4	0.074 (0.071–0.078)	0.277 (0.210–0.345)	0.363 (0.308–0.419)	0.215 (0.202–0.228)	0.455 (0.422–0.488)	0.170 (0.157–0.183)
3-BrC_6H_4	0.026 (0.006–0.046)	0.286 (0.216–0.356)	1.23 (1.09–1.37)	0.191 (0.164–0.218)	0.515 (0.424–0.606)	0.335 (0.289–0.382)
4-BrC_6H_4	0.060 (0.048–0.071)	0.395 (0.269–0.521)	1.86 (1.64–2.08)	0.206 (0.180–0.232)	0.462 (0.362–0.562)	0.381 (0.322–0.441)
3-IC_6H_4	0.077 (0.069–0.086)	0.462 (0.348–0.576)	2.78 (2.37–3.18)	0.214 (0.190–0.237)	0.580 (0.465–0.695)	0.474 (0.404–0.543)
4-IC_6H_4	0.091 (0.066–0.115)	0.426 (0.370–0.482)	2.12 (1.63–2.61)	0.260 (0.189–0.330)	0.722 (0.582–0.863)	0.555 (0.459–0.651)
Saline	0.063 (0.052–0.074)	0.510 (0.443–0.577)	3.99 (3.76–4.22)	—	—	—
Compound I						
0.5 nmol	0.092 (0.074–0.111)	0.364 (0.278–0.449)	1.65 (1.47–1.83)	0.243 (0.205–0.281)	0.674 (0.483–0.865)	0.481 (0.400–0.562)
5 nmol	0.092 (0.078–0.107)	0.356 (0.213–0.500)	0.409 (0.379–0.439)	0.261 (0.214–0.308)	0.659 (0.591–0.727)	0.236 (0.207–0.265)
50 nmol	0.085 (0.071–0.098)	0.346 (0.227–0.465)	0.186 (0.165–0.207)	0.289 (0.244–0.334)	0.389 (0.322–0.457)	0.121 (0.109–0.133)
500 nmol	0.136 (0.097–0.174)	0.296 (0.223–0.369)	0.120 (0.112–0.128)	0.269 (0.243–0.296)	0.092 (0.085–0.099)	0.078 (0.74–0.085)
(*R*)-I, 50 nmol	0.090 (0.067–0.114)	0.458 (0.298–0.619)	0.228 (0.199–0.257)	0.325 (0.250–0.400)	0.378 (0.305–0.451)	0.144 (0.121–0.168)
(*S*)-I, 50 nmol	0.092 (0.075–0.109)	0.571 (0.342–0.801)	3.79 (2.97–4.60)	0.306 (0.243–0.369)	0.601 (0.243–0.369)	0.527 (0.436–0.618)

[a] 50 nmol per animal of each halogenated derivative was coinjected; in the case of I the indicated amount was coinjected; six rats per group.

Table IV—Displacement of (−)-[^{3}H]I by Alkyl Derivatives at 2 h in the Rat

QNB Derivative (R)[a]	Percent of Dose/g (95% Confidence Limits)					
	Blood (B)	Lung	Heart (H)	H/B	Liver	Midbrain
c-C_6H_{11}	0.082 (0.074–0.091)	0.312 (0.236–0.338)	0.398 (0.371–0.426)	4.8	0.266 (0.218–0.314)	0.430 (0.402–0.457)
c-C_5H_9	0.072 (0.061–0.082)	0.319 (0.252–0.386)	0.206 (0.186–0.226)	2.9	0.177 (0.130–0.224)	0.210 (0.188–0.232)
n-C_4H_9	0.076 (0.062–0.091)	0.381 (0.257–0.505)	0.378 (0.281–0.475)	4.9	0.258 (0.181–0.334)	0.336 (0.278–0.393)
Propargyl	0.068 (0.058–0.078)	0.303 (0.251–0.355)	2.68 (2.39–2.97)	39.2	0.222 (0.189–0.255)	0.579 (0.532–0.627)
4-$NH_2C_6H_4$	0.081 (0.072–0.089)	0.423 (0.260–0.587)	1.64 (1.26–2.03)	20.4	0.275 (0.231–0.318)	0.515 (0.420–0.609)
3-Quinuclidinyl xanthene-9-carboxylate	0.063 (0.047–0.078)	0.351 (0.286–0.416)	3.10 (2.79–3.40)	49.4	0.201 (0.167–0.236)	0.526 (0.463–0.590)

[a] 50 nmol of the I derivative per animal was coinjected with 3.5–5 μCi (−)-[^{3}H]I [15–20 μCi/kg]; six rats per group.

Table V—Displacement of (−)-[^{3}H]I by Other Muscarinic Antagonists at 2 h in the Rat

Displacer[a]	Percent of Dose/g (95% Confidence Limits)					
	Blood (B)	Lung	Heart (H)	H/B	Liver	Midbrain
N-Methyl scopolamine	0.074 (0.068–0.081)	0.286 (0.236–0.335)	0.453 (0.400–0.507)	6.1	0.236 (0.207–0.266)	0.641 (0.547–0.736)
Scopolamine	0.104 (0.094–0.114)	0.339 (0.274–0.403)	1.79 (1.53–2.05)	17.2	0.253 (0.227–0.278)	0.546 (0.493–0.599)
Benactyzine	0.062 (0.052–0.072)	0.390 (0.336–0.443)	3.92 (3.53–4.31)	63.2	0.201 (0.165–0.237)	0.542 (0.494–0.590)
4-Bromoatropine	0.061 (0.048–0.074)	0.436 (0.340–0.533)	2.75 (1.49–4.01)	53.3	0.191 (0.165–0.218)	0.517 (0.429–0.605)
Benztropine	0.058 (0.050–0.066)	0.492 (0.399–0.586)	4.31 (3.94–4.67)	74.1	0.177 (0.123–0.231)	0.656 (0.592–0.720)
Carbetapentane	0.048 (0.044–0.053)	0.717 (0.450–0.985)	5.01 (4.62–5.41)	103.2	1.105 (0.091–0.119)	0.507 (0.448–0.566)

[a] 50 nmol of the antagonist per rat was coinjected with 3.5 to 5 μCi (−)-[^{3}H]I [15–20 μCi/kg]; six rats per group.

(RBI). The RBI is defined as the affinity of the analogue (K_h) relative to that of (±)-I as determined by *in vitro* assay, where (±)-I is 100 (Table II). Another advantage of the logit plot is the linear relationship between the logit B/B_0 and the log RBI; this linear relationship allows easier statistical analysis.

Although 50 nmol of each nonradioactive compound (h) was coinjected with the (−)-[^{3}H]I, the actual concentration of material at the receptor site is unknown. The uptake of I in the target tissues is rapid (Table VI), and therefore coinjection of the displacer with the radioligand should allow competitive binding without complications due to differing pharmacokinetics (15). This competition has been demonstrated independently by Maziere *et al.* (16) who showed that atropine could increase the washout of ^{11}C-labeled *N*-methyl-I. If irreversible binding occurred or excretion was faster than rebinding, then these results would not be possible (17). If the concentration of inhibitor is similar, the various compounds should compete with (−)-[^{3}H]I in relation to their affinities for the m-AChR provided that receptor binding is the dominant factor controlling the *in vivo* distribution.

The linear correlation equation for the heart is logit $y = 1.28 - 0.777$ ln RBI ($r^2 = 0.70$) and for the midbrain, logit $y = 3.54 - 0.679$ ln RBI ($r^2 = 0.60$), where logit y is ln $[(B/B_0)/(1 - B/B_0)]$. The correlations are reasonably good

Table VI—Pharmacokinetics of (−)-[^{3}H]I [a]

Time, min	Percent of Dose/g (95% Confidence Limits)				
	Blood	Lung	Heart	Liver	Midbrain
5	0.080 (0.47–0.114)	2.51 (1.85–3.17)	2.53 (1.51–3.56)	0.304 (0.200–0.409)	0.237 (0.147–0.326)
30	0.046 (0.041–0.050)	0.903 (0.751–1.05)	3.54 (2.93–4.16)	0.261 (0.211–0.311)	0.399 (0.270–0.528)
60	0.059 (0.053–0.065)	0.759 (0.615–0.904)	4.12 (3.30–4.93)	0.468 (0.117–1.05)	0.401 (0.319–0.484)
90	0.061 (0.049–0.073)	0.602 (0.535–0.668)	4.43 (3.75–5.12)	0.231 (0.117–0.346)	0.534 (0.425–0.644)
120	0.035 (0.030–0.040)	0.355 (0.296–0.413)	3.16 (2.91–3.41)	0.121 (0.105–0.137)	0.412 (0.353–0.471)

[a] Six rats per group.

considering the assumptions of uniform pharmacokinetics. We suggest that these results, therefore, imply the validity of these assumptions. The *p*-iodo derivative is not as potent as it ought to be based on the correlation in the midbrain (not shown in Fig. 1B, $B/B_0 = 1.07$). This suggests that iodinated I is not as available as the other derivatives for receptor binding in the brain. In general, all iodinated and brominated derivatives lie above the correlation line, indicating that they are not as readily transported to the receptor. However, the high correlation in both the heart and brain indicate that the major factor controlling the *in vivo* distribution in the target organs is the affinity for the m-AChR.

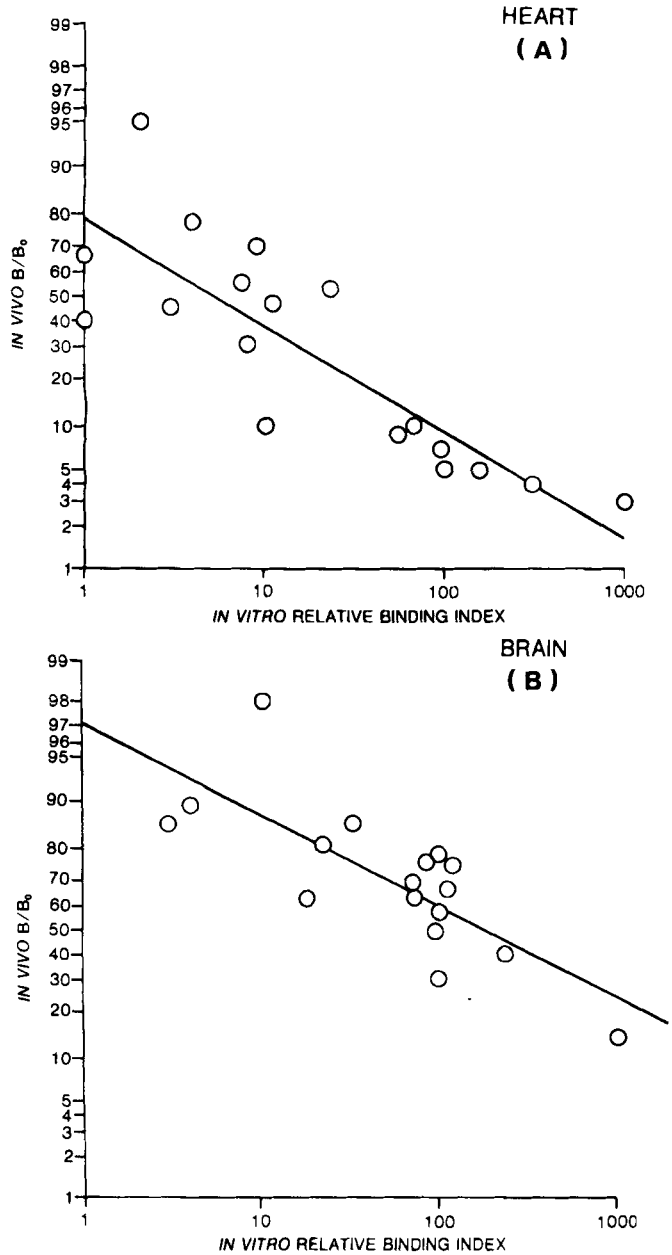

Figure 1—*Plot of logit* B/B_0 *calculated from the ratio of the percent of dose/g bound in the heart (A) and brain (B) in the presence of 50 nmol of nonradioactive analogue per animal to the percent of dose/g bound in the absence of the analogue* versus *the relative bonding index (RBI) determined by* in vitro *assay.*

Relative Displacement in the Heart and Brain—At the same concentration of nonradioactive I, more (−)-[^{3}H]I binding is inhibited in the heart than in the striatum. This could be due to either a higher concentration of m-AChR in the midbrain compared with the heart or to a decreased concentration of nonradioactive compound in the midbrain compared with the heart. From the pharmacokinetic data in Table VI, it is clear that a higher concentration (percent of dose/g) of I is obtained in the heart than in the midbrain by a factor of ≥10 despite the fact that the receptor concentration is considered greater in the striatum (12). Since amines such as I are only transported across the blood–brain barrier as the uncharged species, the differences in uptake between the heart and midbrain could be expected.

The heart-to-blood ratios for (−)-[^{3}H]I (Table VI) are significantly higher than those published for (±)-[^{3}H]I (6, 7). This shows the importance of using the highest affinity stereoisomer of the receptor ligand.

Relative Competition in the Midbrain and Cerebellum—The effect of a difference in m-AChR concentration can best be investigated by comparing the uptake of (−)-[^{3}H]I in the cerebellum and the midbrain (Table III). At maximum specific activity for (−)-[^{3}H]I (33 Ci/mmol), the uptake in the midbrain (MB) and cerebellum (C) is 0.67 and 0.48% of the dose/g, respectively, for a MB/C ratio of 1.40. As the specific activity is decreased by coinjection of I, the percent of dose/g is decreased more rapidly in the cerebellum than in the midbrain. This has the effect of producing higher MB/C ratios as the specific activity is decreased. Finally, with coinjection of 500 nmol of I the ratio is again reduced to 1.2. This can be explained by the cubic equation describing displacement (18):

$$R^2 + R(1 + K^*p^* - K^*q) - K^*q + \frac{hK_h(R+1)R}{(K_h/K^*)R + 1} = 0 \quad \text{(Eq. 2)}$$

where R is the bound/free ratio, K^* is the equilibrium affinity constant of p^*, p^* is the total concentration of radioligand, K_h is the equilibrium affinity constant of h, h is the total concentration of displacer, and q is the total concentration of receptor, provided that the midbrain contains more m-ACh receptor than the cerebellum as the *in vitro* data indicate (12). Examples of the effect of the change in conditions on the bound/free ratio are given in Table VII. It is interesting to note that Yamamura *et al.* (10) using 15 nmol of (±)-[^{3}H]I at 5 Ci/mmol suggested that the MB/C ratio of tritium was indicative of the receptor concentration, but it appears to be fortuitous that the MB/C ratio of 6 approximated the receptor concentration in their experiments. The relative displacement from the two organs appears to be a better explanation than distribution based on receptor concentration. The 2-h distribution of (−)-[^{3}H]I appears to be unrelated to receptor concentration at high specific activity of (−)-[^{3}H]I.

Distribution of Radioiodinated 3-Quinuclidinyl *p*-Iodobenzilate (XVI)—The distribution of XVI labeled with iodine-125 was studied to determine the correlation between the *in vivo* competition study and radiolabeled distribution studies (Table VIII). Four distribution studies at slightly different specific activities show that XVI does give reasonable heart-to-brain (H/B) ratios, but high lung concentration is also evident. The radioactivity is inhibited in the heart and striatum by 50 nmol of I, indicating that XVI is binding to receptor at least in part in these organs. The specific activities were determined by comparing (−)-[^{3}H]I and [^{125}I]XVI binding curves. Setting the receptor concentration equal for both curves permits the calculation of the specific activity of [^{125}I]XVI (19). Another method (20, 21) of adding nonradioactive XII (p) to [^{125}I]XII (p^*) was not sensitive to changes in the specific activity. It is only useful for low specific activity radioligands when the concentration of p and p^* are similar at receptor saturation.

Table VII—Effect of Receptor, Radioligand, and Inhibitor Concentrations on the Bound to Free Drug Ratio (B/F)

	Effect of Concentration on Calculated B/F[a]							
p^*	1.4 nM	1.4 pM	1.4 pM	1.4 nM	1.4 nM	1.4 pM	1.4 pM	1.4 nM
h	25 nM	25 nM	2.5 nM	2.5 nM	25 nM	25 nM	2.5 nM	2.5 nM
q	10 nM	10 nM	10 nM	10 nM	100 nM	100 nM	100 nM	100 nM
B/F								
Calculated	≤1	≤1	96	79	921	938	121	1201
Maximum[b]	125	125	125	125	1250	1250	1250	1250

[a] Calculated from the Cubic Equation (18) using $K^* = 12.5 \times 10^9 M^{-1}$, $K_h = 12.5 \times 10^9 M^{-1}$ for I displacing [^{3}H]I at a typical concentration of p^* (1.4 pM for iodine-125 and 1.4 nM for tritium, h, and q). [b] Calculated from $B/F = K^*q$ (5).

Table VIII—Distribution of 3-Quinuclidinyl-*p*-[^{125}I] Iodobenzilate (XVI)[a]

Displacer	Time, h	Specific Activity, kCi/mol	Percent of Dose/g (95% Confidence Limits)				
			Blood	Lung	Heart	Midbrain	Cerebellum
Saline	0.25	1195	0.118 (0.109-0.128)	5.57 (4.72-6.42)	1.03 (0.782-1.28)	0.222 (0.173-0.271)	0.180 (0.136-0.224)
I[b]	0.25	1195	0.064 (0.056-0.071)	5.66 (4.79-6.54)	0.50 (0.474-0.533)	0.200 (0.142-0.258)	0.156 (0.128-0.185)
Saline	0.25	1214	0.043 (0.035-0.051)	3.93 (2.41-5.45)	0.675 (0.530-0.820)	0.216 (0.182-0.250)	0.150 (0.120-0.179)
Saline	2	1214	0.049 (0.039-0.059)	1.43 (1.00-1.85)	0.274 (0.207-0.342)	0.333 (0.235-0.432)	0.080 (0.055-0.105)
I[b]	2	1214	0.038 (0.035-0.042)	0.961 (0.779-1.14)	0.124 (0.110-0.138)	0.069 (0.064-0.074)	0.030 (0.028-0.033)
Saline	2	—	0.026 (0.024-0.029)	0.977 (0.669-1.28)	0.190 (0.155-0.225)	—	—
I[b]	2	—	0.034 (0.029-0.039)	1.17 (0.922-1.41)	0.142 (0.117-0.167)	—	—
Saline	2	1060	0.038 (0.030-0.047)	1.07 (0.70-1.45)	0.163 (0.117-0.210)	0.176 (0.134-0.219)	0.018 (0.011-0.025)
I[b]	2	1060	0.024 (0.018-0.030)	0.88 (0.55-1.21)	0.094 (0.075-0.112)	0.049 (0.033-0.065)	0.007 (0.002-0.012)

[a] Mixture of four diastereomers. [b] 50 nmol of I per animal coinjected with [^{125}I]XVI; six rats per group.

The higher lipophilicity of XVI when compared with (−)-[^{3}H]I causes higher lung concentration and greater nonreceptor binding to tissue. This may be the cause of the lower displacing power of the nonradioactive compound in the brain. It is also of interest that XVI gives a MB/C ratio of ≥4 at high specific activity. Although it appears that XVI is distributed according to receptor concentration in the brain, recent studies suggest that the ratio is the result of more rapid washout from the cerebellum (9). Using ^{123}I-labeled XVI we were able to visualize the heart and cerebrum of the dog (22). Just as increased uptake in the receptor-containing organs was observed when we used (−)-[^{3}H]I instead of (±)-[^{3}H]I, we also expect in the case of XVI (a mixture of four disastereomers) that the percent of the dose in the receptor-containing organ will increase when the highest affinity isomer is used.

CONCLUSIONS

The *in vivo* displacement experiments show that the relative uptake is correlated with the affinity constant of all derivatives except the *p*-iodo derivative in the brain. The *m*-fluoro derivative is more potent than the *p*-fluoro derivative *in vitro* and *in vivo*. Both bromo derivatives are equally weak receptor binders *in vitro* and *in vivo*. Because of its increased concentration in nontarget organs such as the lung, the *p*-iodo derivative does not inhibit (−)-[^{3}H]I from the midbrain to the same extent as derivatives with comparable m-AChR affinities. Nevertheless, ^{125}I-labeled XVI is taken up by the m-AChR in the heart and brain, although to a lesser extent than (−)-[^{3}H]I. Images of the dog heart and midbrain have been obtained using ^{123}I-labeled XVI (22).

It appears that radioiodinated derivatives are now available for the imaging of β-adrenoceptors in the heart and lung (II) and for the imaging of m-AChR in the heart and brain (XVI). With these agents, changes in receptor concentration as a function of disease may be evaluated *in vivo* (23).

REFERENCES

(1) W. C. Eckelman (Ed.), "Receptor Binding Radiotracers," vols. I and II, CRC Press, Boca Raton, Fla., 1982.

(2) K. D. McElvany, J. A. Katzenellenbogen, S. G. Senderoff, *et al.*, *J. Nucl. Med.*, **22**, P19 (1981).

(3) W. J. Rzeszotarski, R. E. Gibson, W. C. Eckelman, *et al.*, *J. Med. Chem.*, **25**, 1103 (1982).

(4) K. Barovsky and G. Brooker, *J. Cyclic Nucleotide Res.*, **6**, 297 (1980).

(5) W. C. Eckelman, R. C. Reba, R. E. Gibson, *et al.*, *J. Nucl. Med.*, **20**, 350 (1979).

(6) B. E. Francis, W. C. Eckelman, M. Grissom, *et al.*, *Int. J. Nucl. Med. Biol.*, **9**, 173 (1982).

(7) R. E. Gibson, W. C. Eckelman, and F. Vieras, *J. Nucl. Med.*, **20**, 865 (1979).

(8) G. Engel, D. Hoyer, R. Berthold, *et al.*, *NS Arch. Pharmacol.*, **317**, 277 (1981).

(9) R. E. Gibson, E. M. Jagoda, E. M. Weckstein, *et al.*, *J. Nucl. Med.*, **23**, P104 (1982).

(10) H. I. Yamamura, M. J. Kuhar, and S. H. Snyder, *Brain Res.*, **80**, 170 (1974).

(11) H. I. Yamamura and S. H. Snyder, *Mol. Pharmacol.*, **10**, 861 (1974).

(12) R. M. Kobayashi, M. Palkovits, R. E. Hruska, *et al.*, *Brain Res.*, **154**, 13 (1978).

(13) J. A. Fields, W. J. Rocske, E. Morkin, *et al.*, *J. Biol. Chem.*, **253**, 3251 (1978).

(14) D. Rodbard, P. K. Rayford, J. A. Cooper, *et al.*, *J. Clin. Endocrinol.*, **28**, 1412 (1968).

(15) R. J. Tallarida, A. Cowan, and M. W. Adler, *Life Sci.*, **25**, 637 (1979).

(16) M. Maziere, D. Comar, J. M. Godot, *et al.*, *Life Sci.*, **29**, 2391 (1981).

(17) J. J. Frost, "Receptor Binding Radiotracers," vol. II, W. C. Eckelman, Ed., CRC Press, Boca Raton, Fla., 1982, p. 25.

(18) R. P. Ekins, G. B. Newman, and J. L. H. O'Riordan, "In Vitro Studies," R. L. Hayes, Ed., U.S. Atomic Energy Commission, Oak Ridge, Tenn., 1968, p. 59.

(19) R. E. Gibson, W. C. Eckelman, B. E. Francis, *et al.*, *Int. J. Nucl. Med. Biol.*, **9**, 245 (1982).

(20) B. T. Morris, *Clin. Chim. Acta*, **73**, 213 (1976).

(21) J. E. Roulston, *Ann. Clin. Biochem.*, **16**, 26 (1979).

(22) J. J. Conklin, M. P. Grissom, R. R. Eng, *et al.*, *J. Nucl. Med.*, **23**, P22 (1982).

(23) R. E. Gibson, "Receptor Binding Radiotracers," vol. II, W. C. Eckelman, Ed., CRC Press, Boca Raton, Fla., 1982, p. 185.

ACKNOWLEDGMENTS

This work was supported at The George Washington University Medical

Center by Grant No. HL19127 awarded by the Heart, Lung and Blood Institute, at the Armed Forces Radiobiology Research Institute by Research Work Unit 7452-00056 and 7452-00084, and by Grant No. ER60039 awarded by the Department of Energy. We appreciate the technical assistance of Mr. Ralph Will at GWU and E. Barron, N. Fleming, M. Flynn, J. Josza, J. Warrenfeltz, and M. Corral of the AFRRI. Animal research at AFRRI was conducted according to the principles enunciated in the "Guide for the Care and Use of Laboratory Animals," prepared by the Institute of Laboratory Animal Resources, National Research Council.

We would like to thank Dr. Carl Kaiser of Smith Kline and French Laboratories for 4-bromoatropine; Dr. J. W. Bastian of Armour Pharmaceutical Co. for carbetapentane; Dr. W. Bartsch of Boehringer Mannheim for carazolol; and Dr. D. J. Marshall of Ayerst for propranolol. We would also like to thank G. Rosen for preparing the manuscript.

Percutaneous Absorption of Alkanoic Acids I: A Study of Operational Conditions

ZVI LIRON and SASSON COHEN ˣ

Received December 27, 1982, from the *Department of Physiology and Pharmacology, Tel Aviv University, Sackler School of Medicine and Institute for Biological Research, Ness Ziona, Israel.* Accepted for publication October 11, 1983.

Abstract □ The rate of penetration of propionic and butyric acids through excised porcine skin was determined *in vitro* in specific apparatus allowing optimal control of operational conditions. In one technique, the rate was followed by continuous pH-stat titration of acid appearing in the perfusate, in another, by periodic monitoring of [^{14}C]propionic acid in the perfusate. With the assumption that Fick's equation applies to the process of penetration, it was found that the permeability coefficient, K_p, increases with increasing mass of neat penetrant applied per unit area to the donor side, increases with increasing concentration of penetrant in *n*-heptane as vehicle, increases with increasing temperature, E_a = 11.4 kcal/mol, and decreases with decreasing perfusion rate of the acceptor side when this rate is smaller than 60 mL/h.

Keyphrases □ Absorption, percutaneous—alkanoic acids *in vitro*, porcine skin, permeability coefficients, operational conditions □ Alkanoic acids—percutaneous absorption *in vitro*, porcine skin, permeability coefficients, operational conditions □ Permeability coefficients—alkanoic acids through porcine skin, *in vitro* percutaneous absorption, operational conditions

The process of transdermal drug absorption is a subject of current interest in the areas of pharmaceutics, applied pharmacology, and toxicology. For passage through the skin, the penetrating molecule must move first through the stratum corneum, then into the viable epidermis, the papillary dermis, and the capillary walls into the bloodstream. Scheuplein and Blank (1) analyzed the diffusional resistance of the different skin layers, and it was shown clearly that the stratum corneum is overwhelmingly dominant.

This and the passive nature of the stratum corneum enabled application of Fick's equation to the transport process across the skin. A passive system has two main characteristics: (*a*) a delay period following contact of the penetrant with the surface, during which time the membrane itself becomes charged with the penetrant and (*b*) flow across the bulk of the membrane barrier at a steady rate, which lasts as long as the penetrant remains in adequate supply on one side and is being removed from the other. The steady-state flux of penetration, J_s, is given by:

$$J_s = \frac{K_m D(C_I - C_{II})}{X} = K_p \Delta C_s \qquad \text{(Eq. 1)}$$

where $K_p = K_m D/X$. K_p is the permeability coefficient, D is the diffusion coefficient, K_m is the membrane–solution partition coefficient, and X is the thickness of the membrane. ΔC_s expresses the concentration difference under steady-state conditions between the two phases at either side of the membrane. The permeability coefficient, K_p, is physically equivalent to the solute permeability coefficient at zero-volume flow, ω, as shown by Kedem and Katchalsky (2); the relationship is given by $K_p = RT\omega$. It was shown by many workers (1) that Fick's law holds fairly well for skin whether the penetrating substance is a gas, an ion, or a nonelectrolyte.

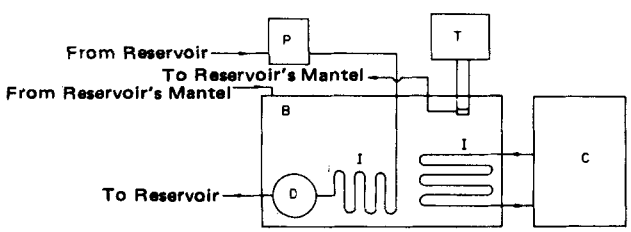

Figure 1—*Schematic representation of the pH-stat assembly. Key: (B) bath; (C) cooler; (D) diffusion cell; (I) immersion coil; (P) peristaltic pump; (T) thermostat.*

For optimal control of operational conditions, the penetration process is usually studied *in vitro*. Excised skin is used in diffusion cells in which a barrier of animal or human skin is interposed between two compartments, and the passage of compounds is measured from the epidermal surface on one side into a bathing fluid on the other side.

The present work is a pilot study of operational factors that affect the percutaneous absorption of propionic and butyric acids through excised porcine skin *in vitro*. Its main objective has been the generation of adequate knowledge to allow a systematic investigation of the permeation process by these and other members of this class of compounds. Concern with the alkanoic acids stems from an interest in the applicability of regular solution theory (3) to pharmaceutical sciences in general and to percutaneous drug application in particular. Recent accurate data (4) on the solubility parameter and molal volumes of a wide range of alkanoic acids suggested their use as candidates of choice in such a study, in preference to other potential permeating species, such as the series of alcohols used by Scheuplein (5). Compliance of the alkanoic acids with this theory is being presented in the second paper of this series (6).

The methodology used in this study is a modified extension of procedures that had been adequately described by earlier workers in this field, notably Ainsworth (7), Blank (8, 9), Wurster and Kramer (10), Scheuplein (5), Polano and Ponec

0022-3549/84/0400-0534$01.00/0